

Ship-Based Measurements of Cloud Optical Properties During the Atlantic Stratocumulus Transition Experiment

A. B. White

Cooperative Institute for Research in Environmental Sciences
University of Colorado at Boulder
National Oceanic and Atmospheric Administration
Boulder, Colorado

C. W. Fairall

National Oceanic and Atmospheric Administration
Environmental Research Laboratories
Environmental Technology Laboratory
Boulder, Colorado

Introduction

The Atlantic Stratocumulus Transition Experiment (ASTEX), conducted in June 1992, was designed with the broad goal of improving the dynamical, radiative, and microphysical models of marine boundary layer (MBL) clouds. This goal was pursued by combining measurements from a number of different platforms including aircraft, satellites, ships, and islands (for more information on ASTEX operations, see Bluth and Albrecht [1992]).

In this paper, we examine the optical properties of MBL clouds using measurements taken on the NOAA research vessel *Malcom Baldrige*. We seek the relationship between optical depth and liquid water because this relationship is used to parameterize the optical properties of clouds in many global climate models (GCMs). We compare our results with the results obtained from two other marine cloud studies.

Analysis of Shipboard Measurements

During ASTEX, scientists from the NOAA/ERL Environmental Technology Laboratory deployed six systems on the *Malcom Baldrige*:

- an air-sea flux and bulk meteorological system

- a ship motion and navigation system
- a lidar ceilometer
- a 915-MHz radar
- a two-channel microwave radiometer
- an Omega-Navaid based rawinsonde system.

Discussion here will be limited to the systems used to provide data for our analysis.

Solar irradiance, R_s , was measured with an Eppley precision pyranometer. We used observations of R_s in cloud-free periods to estimate the clear sky solar curve for the average location of the ship. The transmission coefficient, Tr , was computed as the ratio of R_s to our estimate of the average clear sky value taken from the solar curve. Using Tr and the solar zenith angle, θ , as the input variables, we then used the plane-parallel radiative transfer algorithm of Stephens (1978), as revised by Stephens et al. (1984), to obtain values of albedo, Re , and optical depth, τ .

The Vaisala lidar ceilometer records 30-s profiles of vertical backscatter intensity with 15-m resolution. When a cloud is overhead, the ceilometer returns an estimate of cloud base height. Using this information, we produced values of average cloud fraction, f , measured at zenith (i.e., at $\theta = 0^\circ$).

The NOAA microwave radiometer (Hogg et al. 1983) uses two channels (20 GHz and 31 GHz) for the simultaneous measurement of the column integrated water vapor and liquid water, W . The steerable antenna was pointed to zenith for the duration of ASTEX. Radiometer data were recorded at 30-s resolution.

The time series of shipboard measurements begins on 6 June at 00:00 GMT and ends on 28 June at 06:00 GMT. Much of the data, including surface radiation data, were saved in separate files of 10-min averages and 50-min averages. All other data fields were averaged to match these resolutions.

Cloud Fraction and Zenith Angle Corrections

The Stephens algorithm used to calculate the optical properties R_e and τ is based on the assumption of a horizontally homogenous cloud layer. Although several instances of solid cloud (i.e., $f=1.0$) were observed during ASTEX, the bulk of the data is for broken clouds; the average observed cloud fraction was 0.45. To further complicate matters, the values of f and W were measured using upward-looking instruments (i.e., the ceilometer and radiometer), whereas the values of T_r , R_e , and τ were based on pyranometer measurements that are hemispheric.

In a similar study of broken clouds, Chertock et al. (1993) developed a set of equations (their Model 3) that takes into account cloud fraction and the zenith angle dependence of cloud fraction, $f(\theta)$. Following their notation, the equation for the plane parallel transmission coefficient, T_{pp} , is given by

$$T_{pp} = \frac{T_r - [1 - f(\theta)]}{f(\theta)}$$

The empirical relation used to correct f for zenith angle dependence is taken from Feigelson (1984),

$$f(\theta) = 1 - (1 - f) \exp \{-b f [\sec(\theta) - 1]\}$$

For marine conditions, $b=1$.

Optical Properties

Figure 1 shows the 23-day diurnally averaged optical properties computed from the ASTEX 10-min data. Angle brackets are used to denote a diurnal average. The solid curves are computed directly from the Stephens algorithm and shipboard measurements of f and T_r . Therefore, the

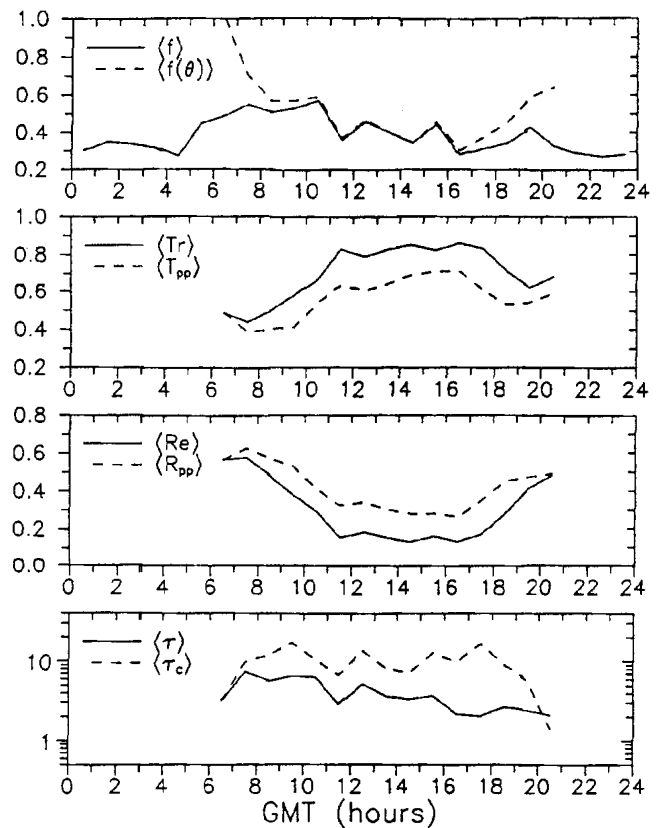


Figure 1. Diurnally averaged optical properties observed during ASTEX. Starting at the top, two curves are given for each of the following: cloud fraction, transmission coefficient, albedo, and optical depth. The solid curves are based on cloud fraction measured at zenith and include the effects of clear sky and clouds. The dashed curves take into account zenith angle variation and differentiate the effects of clouds.

curves for $\langle Tr \rangle$, $\langle Re \rangle$, and $\langle \tau \rangle$ include the combined radiative effects of clear sky and clouds. The dashed curves are computed from the same shipboard measurements of f and Tr modified by Equations (1) and (2). Before averaging, we inserted each 10-min value of T_{pp} into the Stephens algorithm to produce individual time series of plane-parallel albedo, R_{pp} , and cloud optical depth, τ_c . These are the optical properties of the clouds themselves, treated in a plane parallel manner.

We used the diurnal statistics to investigate the relationship between optical depth and liquid water. This relationship is important because it is often used to define the optical properties of clouds in GCMs. For example, Stephens (1978) has shown that $\tau = (3/2)W/(r_e \rho)$, where the effective radius, r_e , is defined as the ratio of the third moment to the second moment of the cloud droplet distribution and ρ is the water density.

The results for ASTEX are shown in Figure 2, along with the results obtained from two other marine cloud studies. Data from the Tropical Instability Wave Experiment (TIWE) (Chertock et al. 1993) is plotted in the same manner as the ASTEX data. The line shows the relationship between τ and W derived from stratocumulus data collected during

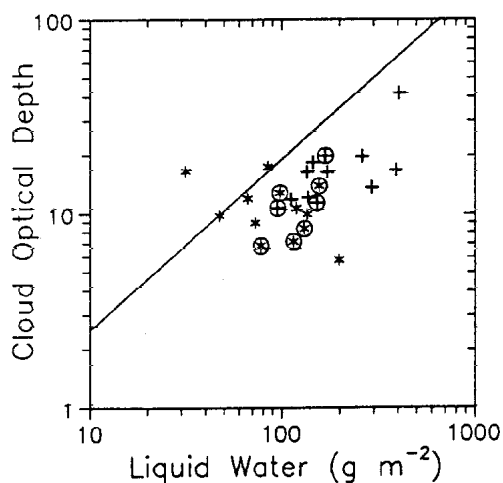


Figure 2. Optical depth versus vertically integrated liquid water. The symbols plot $\langle \tau_c \rangle$ versus $\langle W \rangle$ for ASTEX (asterisks) and TIWE (pluses). The line shows the relationship for FIRE given by Fairall et al. (1990). The circles classify data derived from measurements taken near solar noon ($\theta < 15^\circ$).

the First International Satellite Cloud Climatology Program Regional Experiment (FIRE marine stratocumulus) (Fairall et al. 1990). This relationship was derived for what were essentially plane-parallel clouds (i.e., $f \approx 1.0$), so we expect ASTEX and TIWE data symbols to lie in the neighborhood of the solid line.

The scatter evident in Figure 2 may be attributable to a number of factors. First and foremost is our assumption that we can treat broken clouds in a plane parallel manner. For the case of broken clouds, there is no way to avoid situations where the sun is behind a cloud that is not directly overhead the radiometer. This idea is supported by Figure 2, where data derived from measurements collected near solar noon ($\theta < 15^\circ$) show significantly less scatter than the general population of points. Second, the correction for the zenith angle dependence of cloud fraction given by Equation (2) can produce significant errors at large zenith angles (see Figure 1). These errors will carry through to the estimates of T_{pp} derived from Equation (1). Furthermore, the simple linear partitioning of clear and cloudy regions given by Equation (1) tends to produce erroneous results for cloud fractions less than about 0.1. Finally, there is evidence suggesting that diurnal averages may not be appropriate. For example, measurements of aerosol concentration taken during ASTEX show variability that cannot be characterized as diurnal.

If we consider only the ASTEX and TIWE points derived from measurements taken near solar noon, we can place a line through these points that lies roughly a factor of 2 beneath the FIRE relationship. A study by Albrecht et al. (1990) showed that the marine stratocumulus clouds observed during FIRE contained nearly adiabatic profiles of liquid water. If we assume that the same r_e and droplet concentration, N , can be used to characterize the clouds observed during FIRE, ASTEX, and TIWE, then the near solar noon data in Figure 2 suggest that the ASTEX and TIWE clouds are super-adiabatic.

However, it is possible that r_e and/or N were different for ASTEX and TIWE. For example, FIRE took place much closer to a densely populated coastline than did ASTEX, while TIWE occurred in a pristine marine environment, far away from any continental land mass. Therefore, we might expect FIRE to have a higher mean concentration of aerosols, which would increase N . According to Fairall et al. (1990), τ has a fairly weak dependence on N , $\tau \propto N^{1/3}$.

A factor of two change in the τ versus W relationship would then require a factor of eight change in N or a factor of two change in r_e . Unfortunately, direct measurements of droplet-size distributions are quite rare, making it difficult to evaluate these effects.

Summary

We have provided an analysis of shipboard measurements to estimate the optical properties of marine boundary layer clouds observed during ASTEX. We compared our results with data from two other marine cloud studies, FIRE and TIWE. In our analysis we found that the τ versus W relationship for ASTEX and TIWE was about a factor of two lower in τ than the relationship given for FIRE. We believe that the observed difference may be due to changes in the droplet-size distribution. In the future, we plan to include in our analysis whatever aerosol concentration and/or droplet-size distribution measurements are available.

Acknowledgments

This work was supported by the U.S. Department of Energy's Atmospheric Radiation Measurement Program and the National Oceanic and Atmospheric Administration's Climate and Global Change Program.

References

- Albrecht, B. A., C. W. Fairall, D. W. Thomson, A. B. White, J. B. Snider, and W. H. Schubert. 1990. Surface-based remote sensing of the observed and the adiabatic liquid water content of stratocumulus clouds. *Geophys. Res. Lett.* **17**:89-92.
- Bluth, R. T., and B. A. Albrecht. 1992. Atlantic stratocumulus transition experiment and marine aerosol and gas exchange experiment summary: Part I - Mission summaries. The Pennsylvania State University, Dept. of Meteorology, University Park, Pennsylvania.
- Chertock, B., C. W. Fairall, and A. B. White. 1993. Surface-based measurements and satellite retrievals of broken cloud properties in the Equatorial Pacific. *J. Geophys. Res.* **98**:18,489-18,500.
- Fairall, C. W., J. E. Hare, and J. B. Snider. 1990. An eight-month sample of marine stratocumulus cloud fraction, albedo, and integrated liquid water. *J. Clim.* **3**:847-864.
- Feigelson, E. M. 1984. *Radiation in a Cloudy Atmosphere*. D. Reidel Publishing Co.
- Hogg, D. C., F. O. Guiraud, J. B. Snider, M. T. Decker, and E. R. Westwater. 1983. A steerable dual-channel microwave radiometer for measurement of water vapor and liquid in the atmosphere. *J. Appl. Meteor.* **22**:789-806.
- Stephens, G. L. 1978. Radiation profiles in extended water clouds. II: Parameterization schemes. *J. Atmos. Sci.* **35**:2123-2132.
- Stephens, G. L., S. Ackerman, and E. A. Smith. 1984. A shortwave parameterization revised to improve cloud absorption. *J. Atmos. Sci.* **41**:687-690.